Supplementary Information: **“**Characterization of Organic Aerosol across the Global Remote Troposphere: A comparison of ATom measurements and global chemistry models” by Hodzic et al.

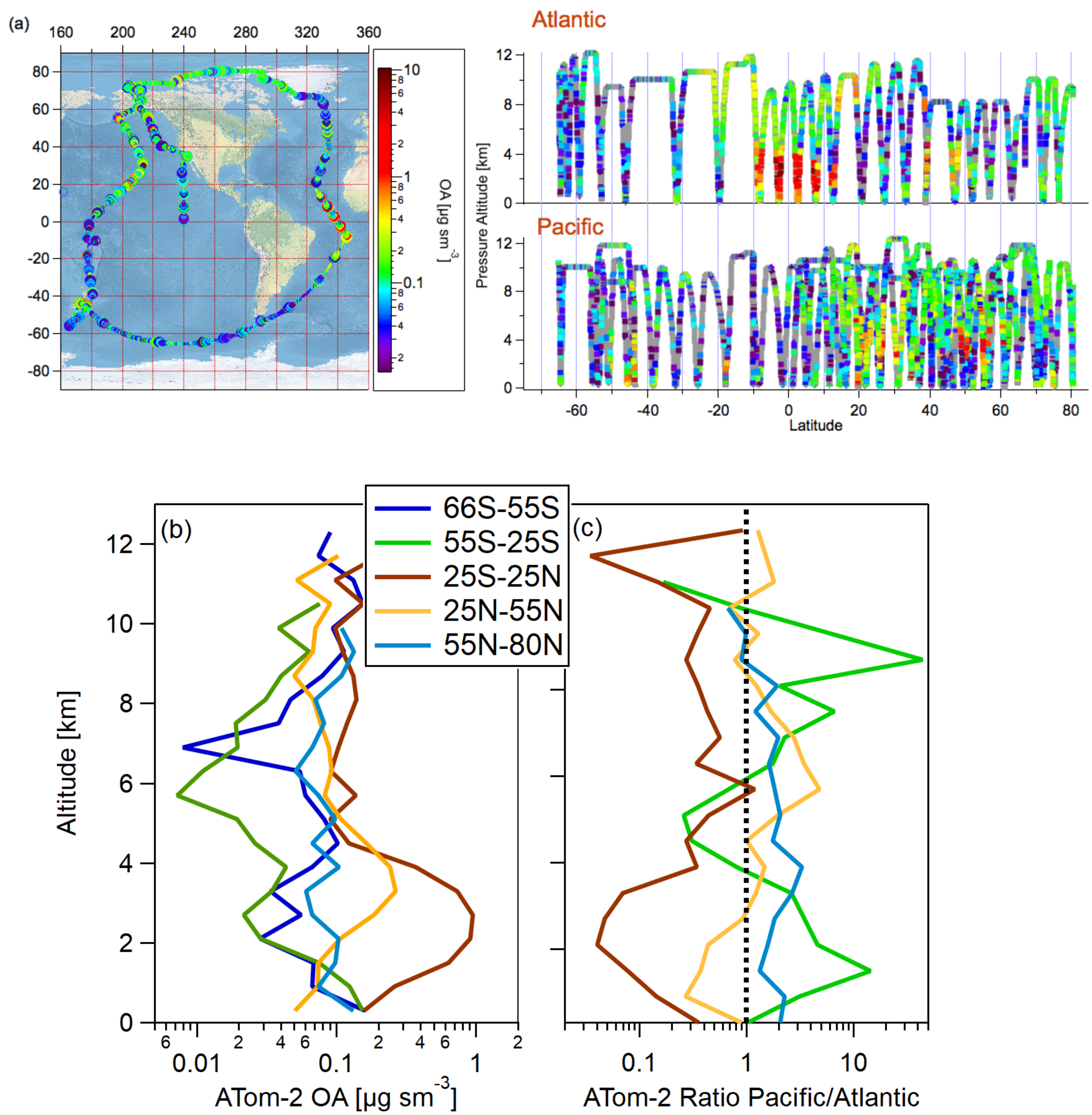

Figure S1: (Upper plots) Vertical distribution of organic aerosol concentrations (OA, µg sm^{-3}) along the ATom-2 flight tracks that took place during February 2017. (Lower plots) The corresponding average OA vertical profiles for each latitude region, and ratios between Pacific and Atlantic OA concentrations in each latitude region.

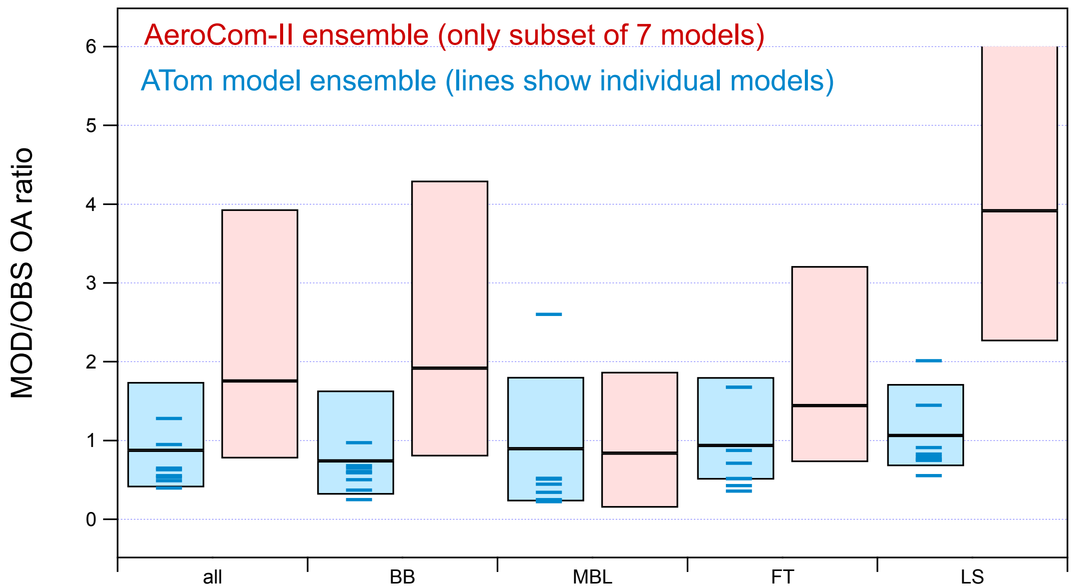

Figure S2: Similar to figure 3, showing the ratios between predicted and observed OA concentrations for all ATom-1 flights as calculated for the ATom model assemble and a subset of AeroCom-II models in different regions. The AeroCom-II subset of models incudes CAM5-MAM3, CCSM4-hem, ECHAM5-HAM2, GEOSChem-APM 8.2, GEOSChem 9, GISS-TOMAS and GMI (see Tsigaridis et al., 2014 for their description).

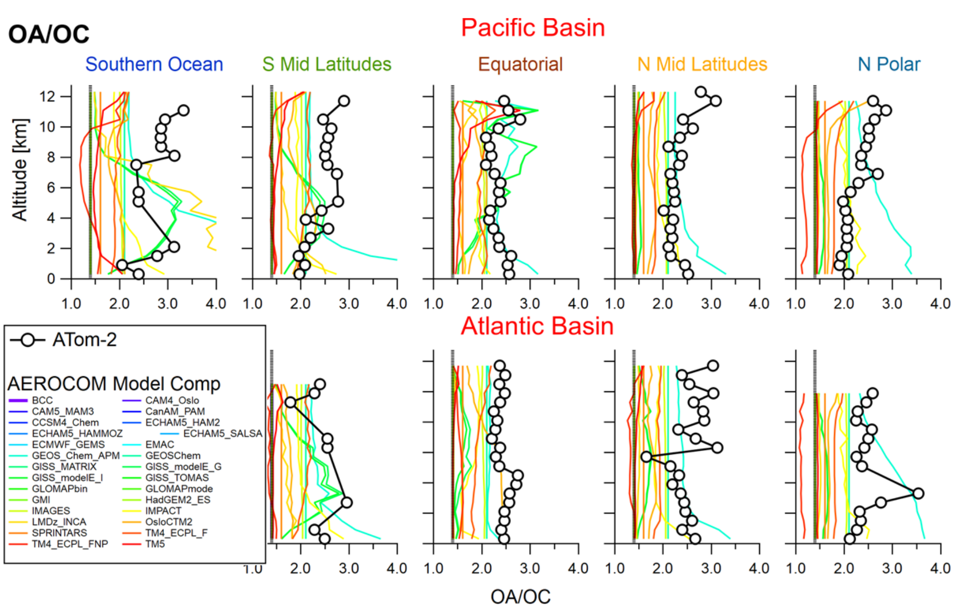

Figure S3: Vertical profiles of OA / OC ratios as measured during the ATom-2 deployment and as calculated in the AeroCom-II models.

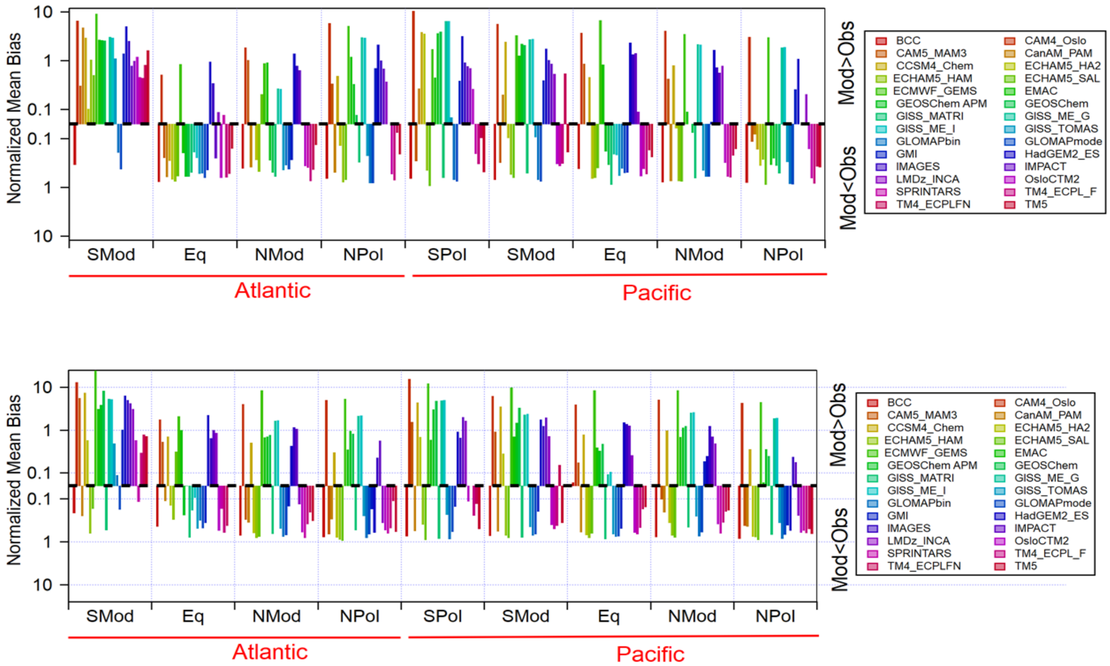

Figure S4: Quantitative comparison of OA measured during ATom-1 (upper panel) and ATom-2 (lower panel) deployments with the average predictions of the AeroCom-II models. The normalized mean bias is shown for all individual model simulations for various latitudinal regions and for both the Atlantic and Pacific basins.

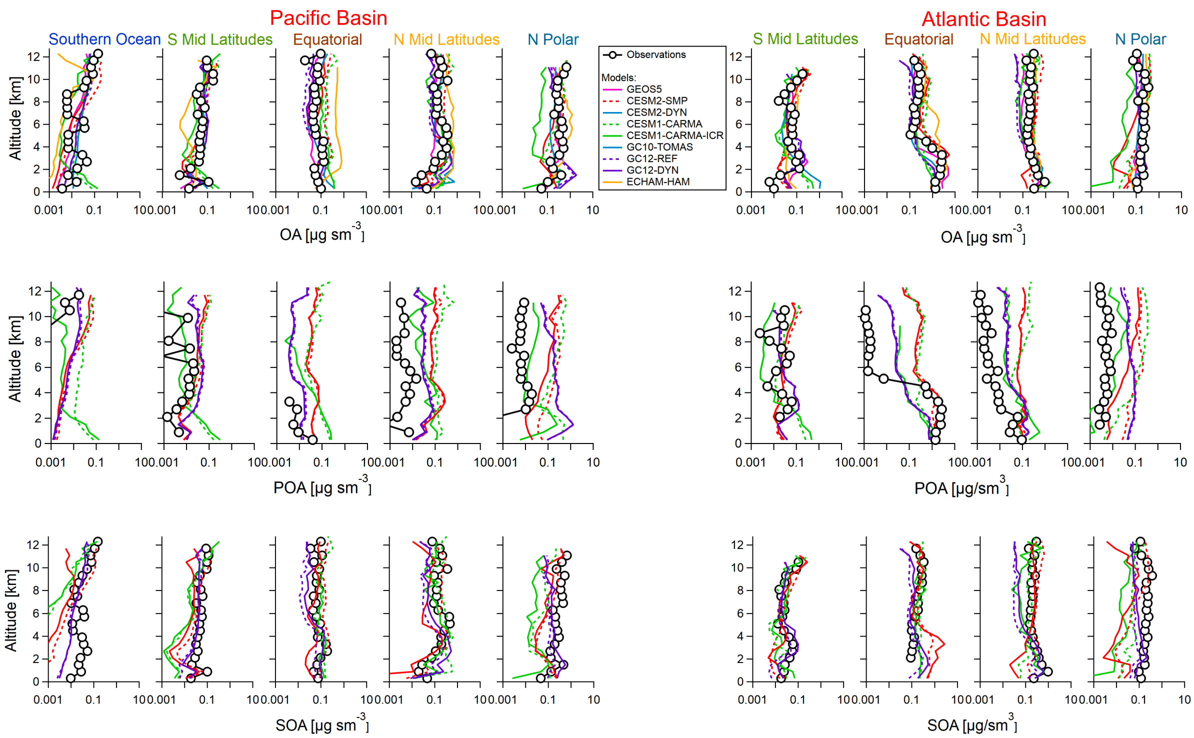

Figure S5: Comparison of latitude-averaged predicted OA, POA and SOA vertical profiles with ATom-1 measurements taken over the Pacific (left side) and the Atlantic basins (right side) for all current model simulations.

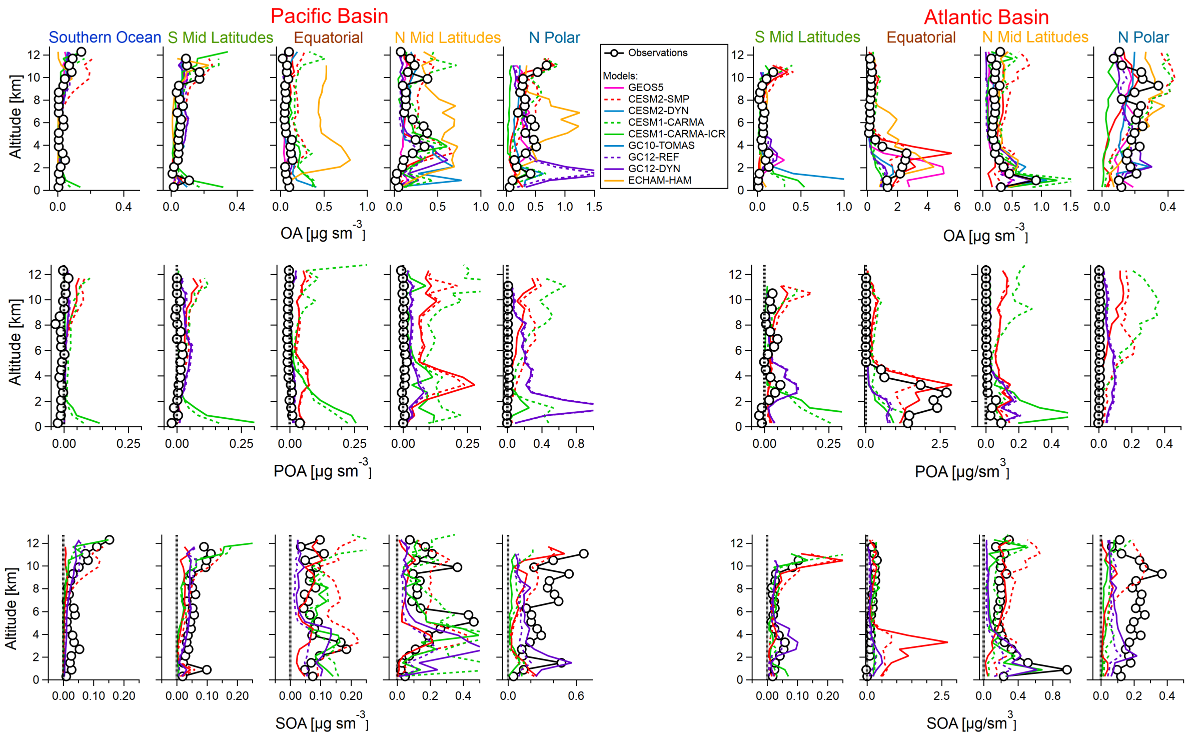

Figure S6: As Figure S5, but showing the plots on a linear scale.

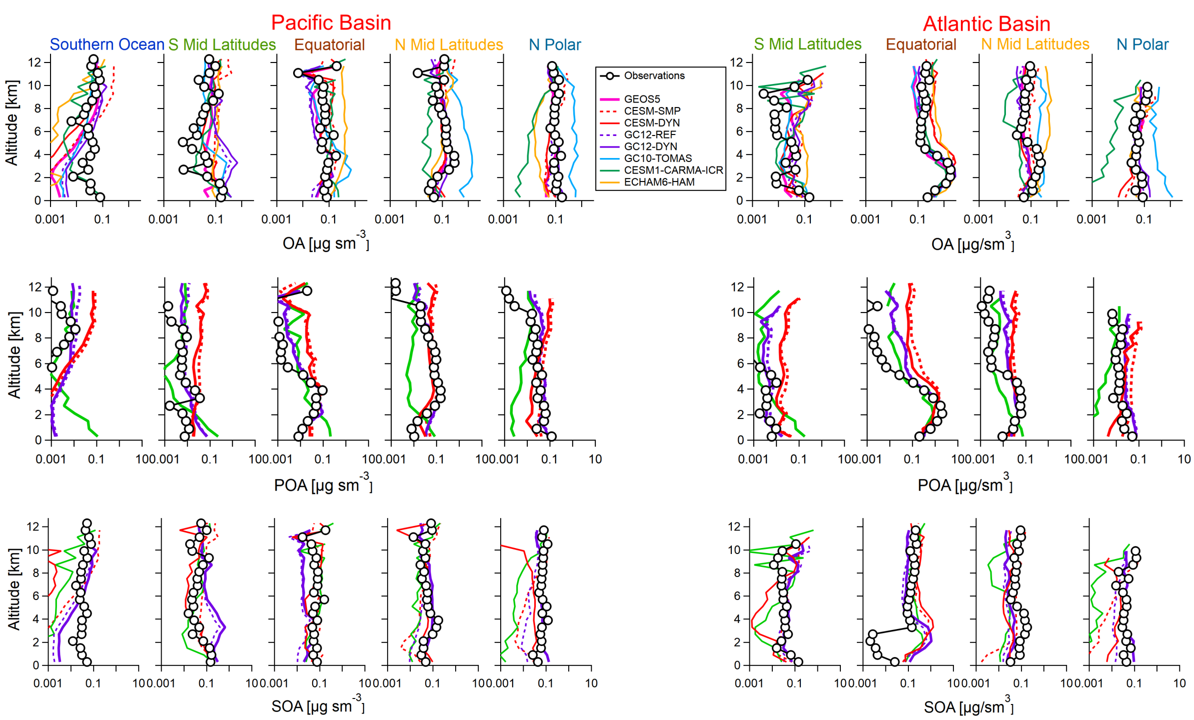

Figure S7: As Figure S5 for ATom-2.

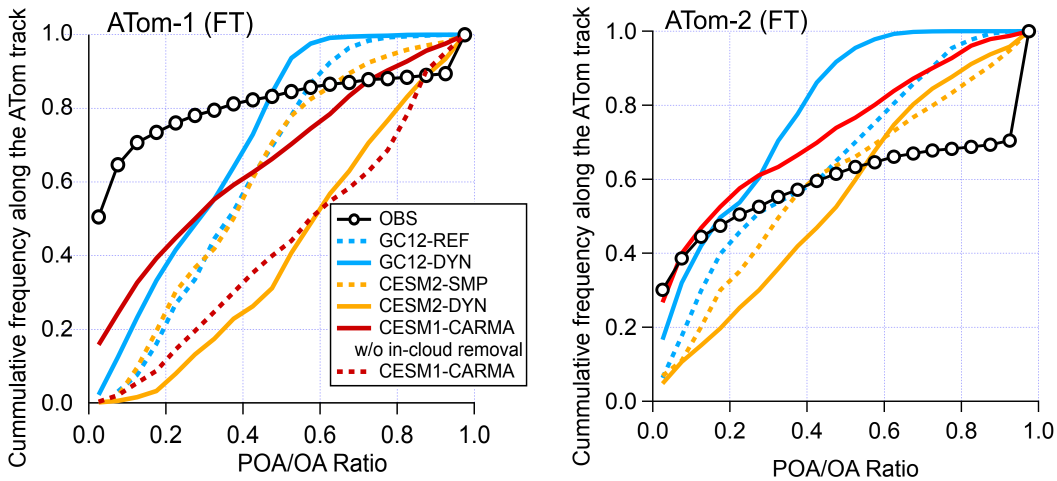

Figure S8: POA/OA distributions (free troposphere only) from Figure 7 shown as cumulative distributions (CDF).

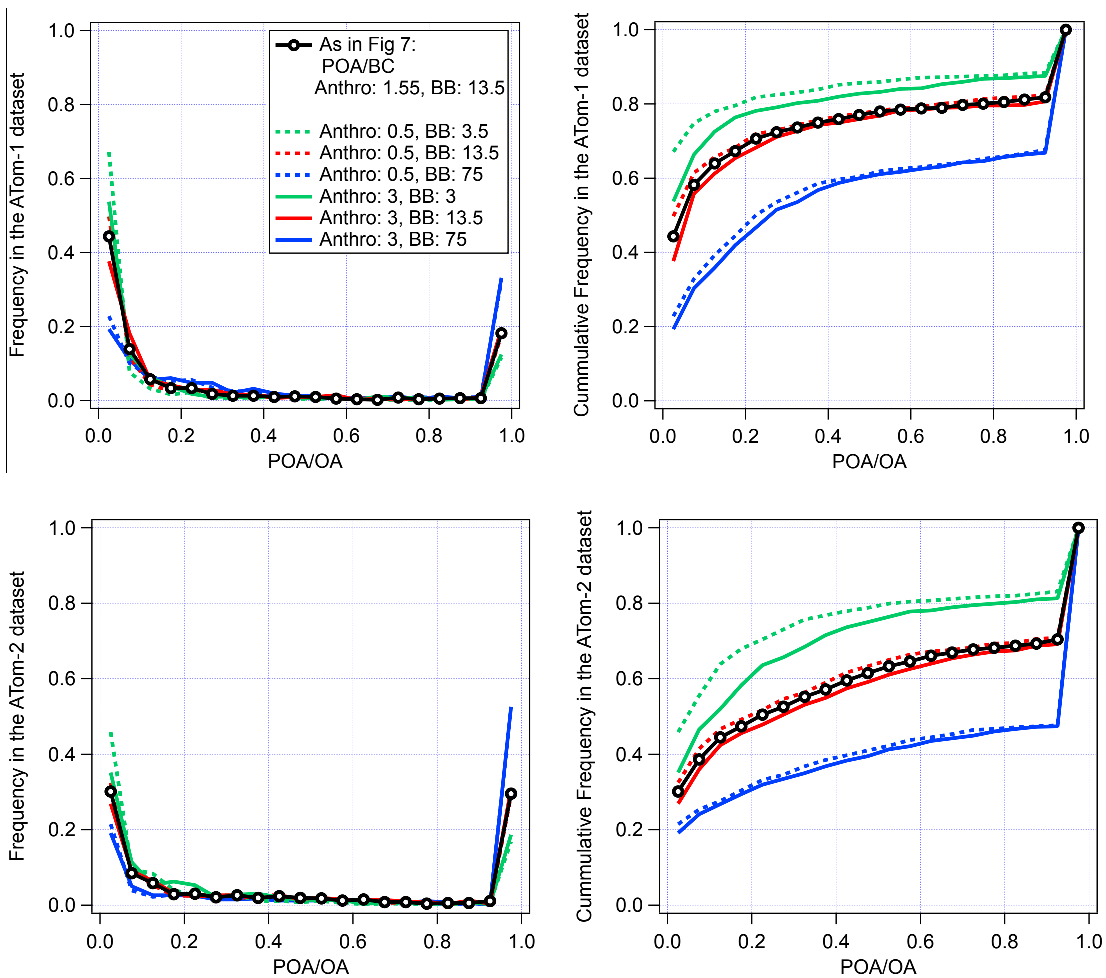

Figure S9: Sensitivity of the overall measured POA/OA distribution to different estimates of POA/BC ratios for both urban and BB sources covering the range of values shown in Table S1 and S2, both for the frequency and cumulative frequency distribution (left/right) and ATom-1 and 2 (top/bottom).

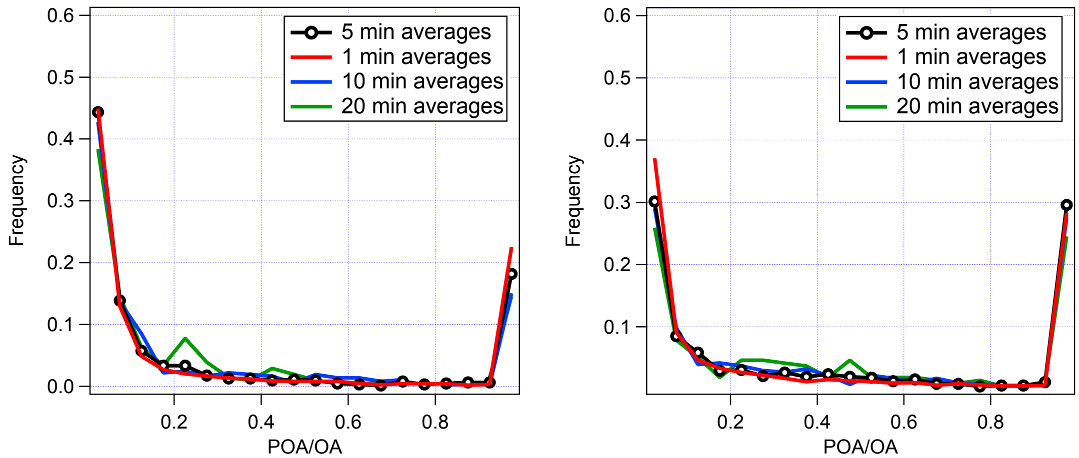

Figure S10: Exploring the impact of OA data below detection limit (DL) and different replacement approaches on the POA/OA distributions in Figure 7 for ATom 1 and 2.

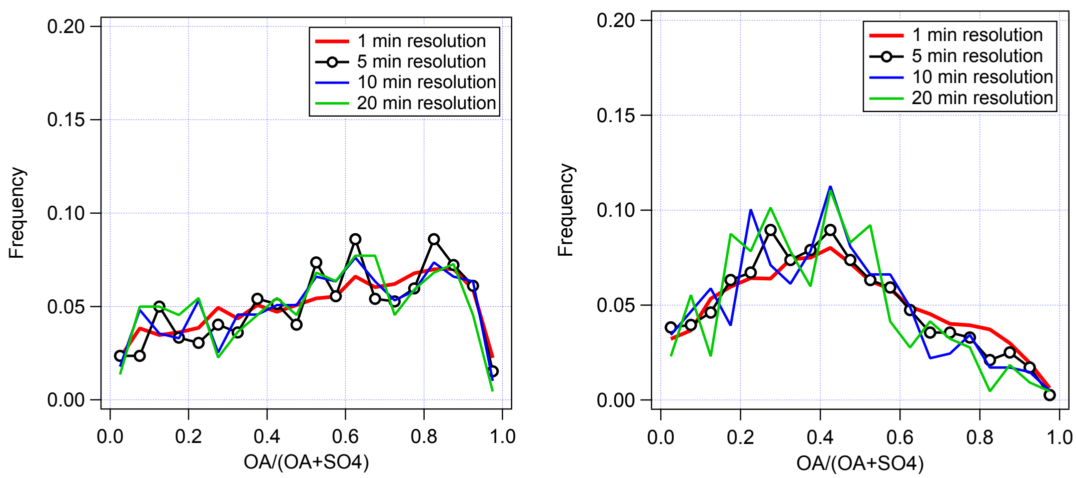

Figure S11: Exploring the impact of various data averaging frequency (from 1 to 20 minute resolutions) on the OA/(OA+SO4) distributions in Figure 9. In the manuscript, a 5-minute averaging is considered.

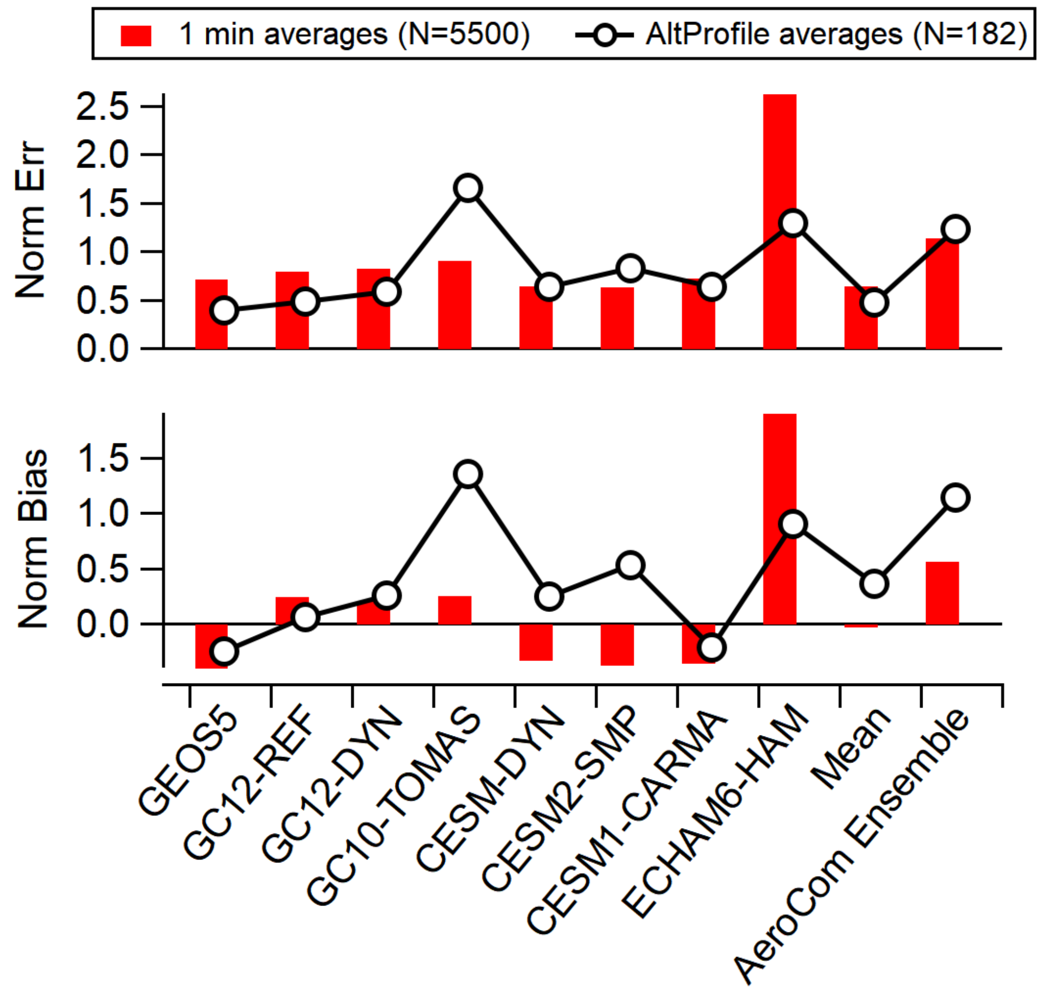

Figure S12: Normalized standard errors and biases calculated for the comparison of the measured and modeled vertical profiles (N=182, 3% of measured points under DL) and the measured and modeled flight racks at 1 min resolution as shown in Table 2 and S3 (N=5580, 32% of measured points under DL) for ATom-2.

Table S1: POA/BC ratios determined in previous field and laboratory emission studies. Studies that reported well constrained POA (up to the double line) were averaged to determine the two values used for $(POA/BC)_{anthro}$ and $(POA/BC)_{BB}$.

Source	Technique	Type of emissions	POA/BC ratio (OA measured)	POA/BC ratio (OC measured, OA/OC of 1.8 used)
Zhang et al, 2005	AMS PCA for POA EC from TOCA	Urban background	1.41	
Szidat et al (2006)	14C source apportionment for EC and OC	Urban mobile sources Residential burning		2.65 11.3
Ban-Weiss et al (2008)	OC: Filters (TOA) Aethelometer and filters for BC	Mobile sources: Light Duty Vehicles Diesel		 2.5 1.3
Aiken et al (2009)	AMS PMF for POA, SP2 for BC	Urban background	0.8	
Christian et al (2010)	TOT EC/OC analyzer	Cooking Stoves Trash Burning Brick Klinn Charcoal Klinn AG Burn		6.3 7.75 0.27 78 200
Chirico et al (2010)	AMS PMF for POA SP2 for BC	Tailpipe emissions, gas vehicle	0.16-0.3	
Minguillon et al (2011)	14C source apportionment for EC and OC, combined with AMS PMF	Urban backg. Rural backg. Biomass burning	 15.4	1.7 4
Huang et al 2012	AMS PMF for POA, SP2 for BC	Urban backg winter Urban backg summer		0.82 1.27
Hayes et al (2013)	AMS PMF for POA, SP2 for BC	Urban background	1.82 (average) 1.51 (more diesel influenced)	
Crippa et al (2013)	AMS PMF for POA, Aethelometer for BC	Urban mobile sources Residential burning	0.5 (ave) 3.4 (ave)	
Huang et al 2014	Offline AMS and TOT OC/EC analyzer, ME2 analysis	Traffic Cooking BB	0.5 2.5 11	

Zhang et al, 2015	14C source apportionment for EC and OC	Fossil fuel, coal burning Residential burning		1.6 8.5
Hu et al, 2016	AMS PMF for POA, SP2 for BC	Urban Background	1.4	
Kim et al, 2018	AMS PMF for POA, SP2 for BC	Urban background (70% HOA, 30% COA)	2.2	
Whatore et al, 2017	TOT EC/OC analyzer	African traditional stoves		4.8
Nault et al, 2018	AMS PMF for POA, SP2 for BC	Urban background	2.38	
Chen et al, 2018	AMS PMF for POA, SP2 for BC	BB urban BB rural	6.25 5	
Chirico et al (2011)	AMS OA SP2 for BC	Tunnel mobile emissions	0.4	
Kim et al, 2017	AMS PMF for POA, SP2 for BC	Total urban POA (40% BB, 27% HOA, 33% COA)	3.2	
Andreae, 2019	Review	Grass burning Tropical forest b Temperate forest b Boreal forest b Peat AG Biofuel Charcoal Average		10.1 15.8 35 25.6 189 21.6 7 18 13.2

Table S2: POA/BC ratios as derived from several emission inventories and as found in published ambient measurements.

Source	**Type of emissions**	**POA/BC ratio (POA=1.4*POC)**	**POA/BC ratio (POA=1.8*POC)**	**Emission year**
Biomass burning Akagi et al. (2011)	Tropical Forest Savanna Crop Residue Pasture Maintenance Extratropical Forest	11.0 9.9 4.3 14.8 22.9	14.2 12.7 5.5 19.1 29.4	N/A

	Peatland	43.6	56.1	
	Chaparral	4.0	5.1	
	Open Cooking	4.9	6.3	
	Stoves	3.6	4.7	
	Charcoal Making	51.8	66.6	
	Charcoal Burning	1.8	2.3	
	Dung Burning	4.8	6.1	
	Garbage Burning	11.4	14.6	
Bond et al. (2004)	Total Fossil fuel	1.1	1.4	1996
	Total Biofuel/Biomass	8.7	11.2	
	Open burning/forest	12.7	16.3	
	Open burning/savanna	9.9	12.7	
	Open burning/crop residue	6.7	8.6	
	Coal/power generation	1.0	1.3	
	Diesel fuel/on-road	0.5	0.7	
	Wood/residential	5.6	7.2	
	Agricultural waste/residential	5.3	6.8	
	Animal waste/residential	5.0	6.5	
	Coal/industry	1.0	1.3	
	Diesel fuel/residential	0.5	0.6	
	Coal/residential	1.2	1.6	
	Diesel fuel/off-road	0.7	0.9	
	Gasoline/transport	10.1	13.0	
	Other combustion	2.3	2.9	
CEDS inventory (CMIP 6)	Energy	2.4	3.1	2014
	Transportation	0.6	0.8	
	Ships	1.1	1.4	
	Residential	4.2	5.4	
	Industrial process	2.5	3.2	
	Waste	8.7	11.2	
	Total	3.4	4.4	
ACCLIP	Energy	9.6	12.3	2000
	Transportation	1.5	1.9	
	Industries	2.1	2.7	
	Residential	5.6	7.2	
	Agricultural waste	6.7	8.6	
	Waste	1.9	2.4	
	Total	3.5	4.5	
EDGAR v4.3.2	Aviation climbing and descent	0.7	0.9	2012
	Aviation cruise	0.7	0.9	
	Aviation landing and take off	0.7	0.9	
	Oil refineries and Transformation	0.2	0.3	
	Energy industry	1.6	2.1	
	Combustion in manufacturing industry	2.7	3.4	
	Fuel exploitation	0.1	0.2	
	Non-road ground transportation	1.5	1.9	

	Ships	0.7	0.9	
	Road transportation	1.1	1.4	
	Residential and other sectors	5.4	6.9	
	Agricultural waste burning	21.0	27.0	
	Waste incineration	2.4	3.1	
	Fossil Fuel fires	0.7	0.9	
	Total	3.5	4.5	

Table S3: Similar to table 2 but for sulfate aerosols. The statistical indicators are calculated as normalized mean bias $NMB(\%) = 100 \times \sum_i (M_i - O_i) / \sum_i O_i$; normalized mean error $NME(\%) = 100 \times \sum_i |(M_i - O_i)| / \sum_i O_i$; root mean square error $RMSE(\mu g\ m^{-3}) = \sqrt{(1/N) \sum_i (M_i - O_i)^2}$ and correlation coefficient (R^2) between modeled (M_i) and observed (O_i) data points. The mean of ATom-1 sulfate observations is ~0.18 μg m^{-3} and for ATom-2 is ~0.165 μg m^{-3}.

Sulfate	Avg.Mod. (μg m^{-3})	NMB (%)	NME (%)	RMSE (μg m^{-3})	R^2	Avg.Mod. (μg m^{-3})	NMB (%)	NME (%)	RMSE (μg m^{-3})	R^2
Model	*ATom-1 scores (August 2016)*					*ATom-2 scores (February 2017)*				
ATom Ensemble	0.188	-0.31	73.8	0.446	0.21	0.163	-3.3	65.2	0.234	0.20
CESM2-DYN	0.197	2.3	86.0	0.471	0.16	0.113	-33.6	65.2	0.322	0.15
CESM2-SMP	0.190	-1.1	85.3	0.475	0.15	0.106	-38.0	64.1	0.306	0.23
CESM1-CARMA	0.161	-11.0	89.4	0.455	0.12	0.106	-36.4	72.9	0.420	0.05
ECHAM6-HAM	0.518	190	263	0.785	0.03	0.471	191.5	262.8	0.634	0.01
GC12-DYN	0.205	13.4	79.6	0.413	0.24	0.216	21.0	82.5	0.251	0.15
GC12-REF	0.211	16.9	80.9	0.414	0.24	0.222	24.4	79.5	0.245	0.17
GC10-TOMAS	0.202	8.2	85.6	0.445	0.15	0.211	25.9	91.1	0.289	0.04
GEOS5-GOCART	0.110	-43.2	69.1	0.468	0.11	0.103	-40.6	71.9	0.237	0.10

References:

Aiken, a. C., Salcedo, D., Cubison, M. J., Huffman, J. a., DeCarlo, P. F., Ulbrich, I. M., Docherty, K. S., Sueper, D., Kimmel, J. R., Worsnop, D. R., Trimborn, A., Northway, M., Stone, E. a., Schauer, J. J., Volkamer, R. M., Fortner, E., de Foy, B., Wang, J., Laskin, A., Shutthanandan, V., Zheng, J., Zhang, R., Gaffney, J., Marley, N. a., Paredes-Miranda, G., Arnott, W. P., Molina, L. T., Sosa, G. and Jimenez, J. L.: Mexico City aerosol analysis during MILAGRO using high resolution aerosol mass spectrometry at the urban supersite (T0) – Part 1: Fine particle composition and organic source apportionment, Atmos. Chem. Phys., 9(17), 6633–6653, doi:10.5194/acp-9-6633-2009, 2009.

Andreae, M. O.: Emission of trace gases and aerosols from biomass burning – An updated assessment, Atmos. Chem. Phys. Discuss., 1–27, doi:10.5194/acp-2019-303, 2019.

Ban-Weiss, G. A., McLaughlin, J. P., Harley, R. A., Lunden, M. M., Kirchstetter, T. W., Kean, A. J., Strawa, A. W., Stevenson, E. D. and Kendall, G. R.: Long-term changes in emissions of nitrogen oxides and particulate matter from on-road gasoline and diesel vehicles, Atmos. Environ., 42(2), 220–232, doi:10.1016/j.atmosenv.2007.09.049, 2008.

Chen, C. L., Chen, S., Russell, L. M., Liu, J., Price, D. J., Betha, R., Sanchez, K. J., Lee, A. K. Y., Williams, L., Collier, S. C., Zhang, Q., Kumar, A., Kleeman, M. J., Zhang, X. and Cappa, C. D.: Organic Aerosol Particle Chemical Properties Associated With Residential Burning and Fog in Wintertime San Joaquin Valley (Fresno) and With Vehicle and Firework Emissions in Summertime South Coast Air Basin (Fontana), J. Geophys. Res. Atmos., 123(18), 10,707-10,731, doi:10.1029/2018JD028374, 2018.

Chirico, R., DeCarlo, P. F., Heringa, M. F., Tritscher, T., Richter, R., Prévôt, A. S. H., Dommen, J., Weingartner, E., Wehrle, G., Gysel, M., Laborde, M. and Baltensperger, U.: Impact of aftertreatment devices on primary emissions and secondary organic aerosol formation potential from in-use diesel vehicles: results from smog chamber experiments, Atmos. Chem. Phys., 10(23), 11545–11563, doi:10.5194/acp-10-11545-2010, 2010.

Chirico, R., Prevot, A. S. H., DeCarlo, P. F., Heringa, M. F., Richter, R., Weingartner, E. and Baltensperger, U.: Aerosol and trace gas vehicle emission factors measured in a tunnel using an Aerosol Mass Spectrometer and other on-line instrumentation, Atmos. Environ., 45(13), 2182–2192, doi:10.1016/j.atmosenv.2011.01.069, 2011.

Christian, T. J., Yokelson, R. J., Cárdenas, B., Molina, L. T., Engling, G. and Hsu, S.-C.: Trace gas and particle emissions from domestic and industrial biofuel use and garbage burning in central Mexico, Atmos. Chem. Phys., 10(2), 565–584, doi:10.5194/acp-10-565-2010, 2010.

Goetz, J. D., Giordano, M. R., Stockwell, C. E., Christian, T. J., Maharjan, R., Adhikari, S., Bhave, P. V, Praveen, P. S., Panday, A. K., Jayarathne, T., Stone, E. A., Yokelson, R. J. and DeCarlo, P. F.: Speciated online PM1 from South Asian combustion sources – Part

1: Fuel-based emission factors and size distributions, Atmos. Chem. Phys., 18(19), 14653–14679, doi:10.5194/acp-18-14653-2018, 2018.

Haslett, S. L., Thomas, J. C., Morgan, W. T., Hadden, R., Liu, D., Allan, J. D., Williams, P. I., Keita, S., Liousse, C. and Coe, H.: Highly controlled, reproducible measurements of aerosol emissions from combustion of a common African biofuel source, Atmos. Chem. Phys., 18(1), 385–403, doi:10.5194/acp-18-385-2018, 2018.

Hayes, P. L., Ortega, A. M., Cubison, M. J., Froyd, K. D., Zhao, Y., Cliff, S. S., Hu, W. W., Toohey, D. W., Flynn, J. H., Lefer, B. L., Grossberg, N., Alvarez, S., Rappenglück, B., Taylor, J. W., Allan, J. D., Holloway, J. S., Gilman, J. B., Kuster, W. C., de Gouw, J. A., Massoli, P., Zhang, X., Liu, J., Weber, R. J., Corrigan, A. L., Russell, L. M., Isaacman, G., Worton, D. R., Kreisberg, N. M., Goldstein, A. H., Thalman, R., Waxman, E. M., Volkamer, R., Lin, Y. H., Surratt, J. D., Kleindienst, T. E., Offenberg, J. H., Dusanter, S., Griffith, S., Stevens, P. S., Brioude, J., Angevine, W. M. and Jimenez, J. L.: Organic aerosol composition and sources in Pasadena, California, during the 2010 CalNex campaign, J. Geophys. Res. Atmos., 118(16), 9233–9257, doi:10.1002/jgrd.50530, 2013.

Huang, R. J., Zhang, Y., Bozzetti, C., Ho, K. F., Cao, J. J., Han, Y., Daellenbach, K. R., Slowik, J. G., Platt, S. M., Canonaco, F., Zotter, P., Wolf, R., Pieber, S. M., Bruns, E. A., Crippa, M., Ciarelli, G., Piazzalunga, A., Schwikowski, M., Abbaszade, G., Schnelle-Kreis, J., Zimmermann, R., An, Z., Szidat, S., Baltensperger, U., El Haddad, I. and Prévôt, A. S. H.: High secondary aerosol contribution to particulate pollution during haze events in China, Nature, 514(7521), 218–222, doi:10.1038/nature13774, 2015.

Huang, X. F., Xue, L., Tian, X. D., Shao, W. W., Sun, T. Le, Gong, Z. H., Ju, W. W., Jiang, B., Hu, M. and He, L. Y.: Highly time-resolved carbonaceous aerosol characterization in Yangtze River Delta of China: Composition, mixing state and secondary formation, Atmos. Environ., 64, 200–207, doi:10.1016/j.atmosenv.2012.09.059, 2013.

Kim, H., Zhang, Q. and Heo, J.: Influence of intense secondary aerosol formation and long-range transport on aerosol chemistry and properties in the Seoul Metropolitan Area during spring time: Results from KORUS-AQ, Atmos. Chem. Phys., 18(10), 7149–7168, doi:10.5194/acp-18-7149-2018, 2018.

Kim, H., Zhang, Q., Bae, G.-N., Kim, J. Y. and Lee, S. B.: Sources and atmospheric processing of winter aerosols in Seoul, Korea: insights from real-time measurements using a high-resolution aerosol mass spectrometer, Atmos. Chem. Phys., 17(3), 2009–2033, doi:10.5194/acp-17-2009-2017, 2017.

Minguillon, M. C., Perron, N., Querol, X., Szidat, S., Fahrni, S. M. M., Alastuey, A., Jimenez, J. L. L., Mohr, C., Ortega, A. M. M., Day, D. A. A., Lanz, V. A. A., Wacker, L., Reche, C., Cusack, M., Amato, F., Kiss, G., Hoffer, A., Decesari, S., Moretti, F., Hillamo, R., Teinila, K., Seco, R., Penuelas, J., Metzger, A., Schallhart, S., Muller, M., Hansel, A., Burkhart, J. F. F., Baltensperger, U., Prevot, A. S. H., Minguillón, M. C., Perron, N., Querol, X., Szidat, S., Fahrni, S. M. M., Alastuey, A., Jimenez, J. L. L., Mohr, C., Ortega, A. M. M., Day, D. A. A., Lanz, V. A. A., Wacker, L., Reche, C., Cusack, M., Amato, F., Kiss, G., Hoffer, A., Decesari, S., Moretti, F., Hillamo, R., Teinilä, K., Seco, R., Peñuelas, J., Metzger, A., Schallhart, S., Müller, M., Hansel, A., Burkhart, J. F. F., Baltensperger, U. and Prévót, A. S. H.: Fossil versus contemporary sources of fine elemental and organic carbonaceous particulate matter during the DAURE campaign in Northeast Spain, Atmos. Chem. Phys., 11(23), 12067–12084, doi:doi:10.5194/acp-11-12067-2011, 2011.

Nault, B. A., Campuzano-Jost, P., Day, D. A., Schroder, J. C., Anderson, B., Beyersdorf, A. J., Blake, D. R., Brune, W. H., Choi, Y., Corr, C. A., de Gouw, J. A., Dibb, J., DiGangi, J. P., Diskin, G. S., Fried, A., Huey, L. G., Kim, M. J., Knote, C. J., Lamb, K. D., Lee, T., Park, T., Pusede, S. E., Scheuer, E., Thornhill, K. L., Woo, J.-H. and Jimenez, J. L.: Secondary organic aerosol production from local emissions dominates the organic aerosol budget over Seoul, South Korea, during KORUS-AQ, Atmos. Chem. Phys., 18(24), 17769–17800, doi:10.5194/acp-18-17769-2018, 2018.

Shen, G., Wei, S., Wei, W., Zhang, Y., Min, Y., Wang, B., Wang, R., Li, W., Shen, H., Huang, Y., Yang, Y., Wang, W., Wang, X., Wang, X. and Tao, S.: Emission factors, size distributions, and emission inventories of carbonaceous particulate matter from residential wood combustion in rural china, Environ. Sci. Technol., 46(7), 4207–4214, doi:10.1021/es203957u, 2012.

Shen, G., Xue, M., Chen, Y., Yang, C., Li, W., Shen, H., Huang, Y., Zhang, Y., Chen, H., Zhu, Y., Wu, H., Ding, A. and Tao, S.: Comparison of carbonaceous particulate matter emission factors among different solid fuels burned in residential stoves, Atmos. Environ., 89, 337–345, doi:10.1016/j.atmosenv.2014.01.033, 2014.

Szidat, S., Jenk, T. M., Synal, H. A., Kalberer, M., Wacker, L., Hajdas, I., Kasper-Giebl, A. and Baltensperger, U.: Contributions of fossil fuel, biomass-burning, and biogenic emissions to carbonaceous aerosols in Zurich as traced by 14C, J. Geophys. Res. Atmos., 111(7), 1–12, doi:10.1029/2005JD006590, 2006.

Wathore, R., Mortimer, K. and Grieshop, A. P.: In-Use Emissions and Estimated Impacts of Traditional, Natural- and Forced-Draft Cookstoves in Rural Malawi, Environ. Sci. Technol., 51(3), 1929–1938, doi:10.1021/acs.est.6b05557, 2017.

Zhang, Y.-L., Huang, R.-J., El Haddad, I., Ho, K.-F., Cao, J.-J., Han, Y., Zotter, P., Bozzetti, C., Daellenbach, K. R., Canonaco, F., Slowik, J. G., Salazar, G., Schwikowski, M., Schnelle-Kreis, J., Abbaszade, G., Zimmermann, R., Baltensperger, U., Prévôt, A. S. H. and Szidat, S.: Fossil vs. non-fossil sources of fine carbonaceous aerosols in four Chinese cities during the extreme winter haze episode of 2013, Atmos. Chem. Phys., 15(3), 1299–1312, doi:10.5194/acp-15-1299-2015, 2015.